

Combined Use of Kinetic and Crystallographic Data to Probe the Hydrolysis of a Simple Amide

Patrick Camilleri,* Joseph V. Carey, and Barbara Odell

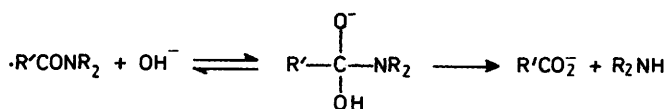
Shell Research Limited, Sittingbourne Research Centre, Sittingbourne, Kent ME9 8AG

David J. Williams

Department of Chemistry, Imperial College, London SW7 2AY

The base-catalysed hydrolysis of the formyl derivative of a nitromethylene heterocycle is described. A Brønsted plot of the data gives $\beta = 0.56$. The point for water falls on the Brønsted line, which indicates that the water-catalysed hydrolysis involves a transition state in which one molecule of water, acting as a base, abstracts a proton from a nucleophilic water molecule. This result is supported by proton inventory studies. We have also analysed the crystal structures of the amide and of its product of hydrolysis and have identified structural features that are thought to be responsible for facile hydrolysis.

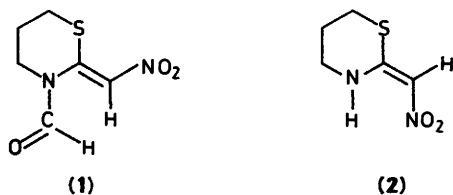
Most simple amides¹ hydrolyse in alkaline media at a slower rate than the corresponding esters. The mechanism of hydrolysis of an amide under these conditions usually involves nucleophilic addition to the carbonyl function, leading to the formation of a tetrahedral intermediate.



In addition to the hydroxide ion-induced hydrolysis, cleavage of the amide bond can also occur *via* general base catalysis. Such a mechanism is normally observed in the case of reactive molecules such as *N*-acetylimidazole² or *N*-methyl-2,2,2-trifluoroacetanilide,³ where hydrolysis is accelerated under basic and neutral conditions by species such as acetate, phosphate, and hydrogencarbonate. In the case of *N*-acetylimidazole enhanced reactivity has been explained² as being due to the electron pair on the nitrogen in the amide group being involved in resonance with the aromatic ring rather than with the carbonyl group; this leads to a weakening of the carbon–nitrogen bond, which then becomes more sensitive to hydrolysis.

The electron-withdrawing nature of the fluorine atoms in *N*-methyl-2,2,2-trifluoroacetanilide leads to a lowering of the electron density at the carbonyl carbon, making it again more susceptible to nucleophilic attack.

In the present study we report the base-catalysed hydrolysis of 3-formyl-2-nitromethylenetetrahydro-2*H*-1,3-thiazine (1) to give the corresponding amine (2). Kinetic evidence is presented that implicates nucleophilic attack by water and base.



We have also examined the crystal structures of (1) and (2) to help in our understanding of the reaction pathway and to identify structural features that most probably lead to the facile hydrolysis of (1).

Experimental

Materials.—Samples of (1) and (2) were obtained from the Analytical Chemical Division at Shell Research Ltd.,

Sittingbourne. Inorganic reagents and buffer components were of analytical grade. Water was distilled deionised millipore quality. D₂O was obtained from Nuclear Resonance Limited and was ≥ 99.6 atom %D.

Kinetic Measurements.—Reactions were followed using 1 cm quartz cuvettes, placed in a thermostatted cell holder of a Beckman Model DV-8 u.v.–visible spectrophotometer. The hydrolysis of (1) was monitored at a wavelength of 340 nm. Kinetics were performed at an ionic strength of 1.0, adjusted with potassium chloride. Buffers used were formate (pH 3.8–4.8), acetate (pH 4.2–5.6), phosphate (pH 6.2–7.2), imidazole (pH 6.4–8.2), *N*-methylimidazole (pH 6.5–8.3), and borate (pH 8.7–9.5).

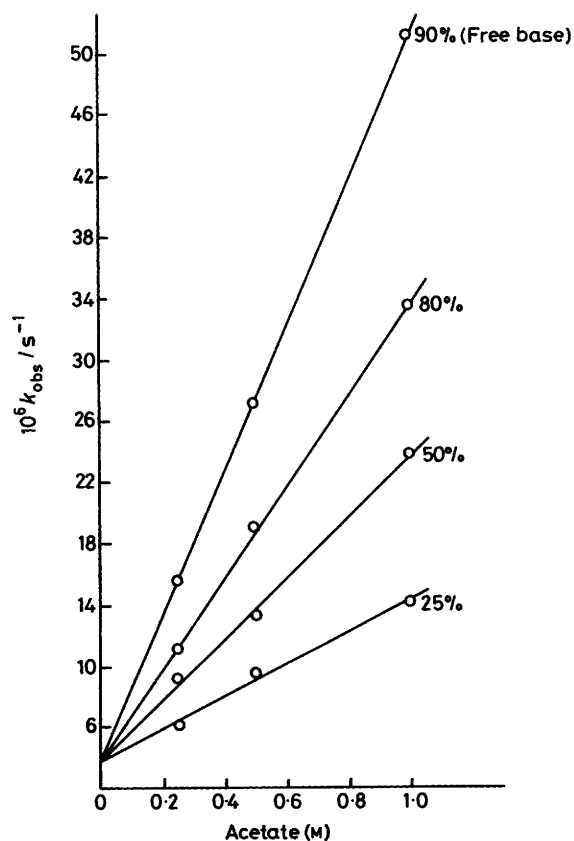


Figure 1. Catalysis by acetate buffer

An aliquot (2 ml) of buffer solution of known pH was placed in the cuvette and left to equilibrate at 25 °C. A stock solution of (1) (2 μ l, $\approx 10^{-2}$ M) in dioxane was then introduced and the cuvette shaken to ensure thorough mixing. The reaction was followed for at least three half-lives. The first-order rate constants were calculated after the infinity absorbance values were measured. The pH at the end of the reaction was also measured and this did not change more than ± 0.03 of a pH unit.

H.p.l.c. analysis [Zorbax ODS column: 25 cm \times 4.5 mm (i.d.); acetonitrile–water (40:60); flow rate 1 ml min $^{-1}$] of the product of reaction revealed that the hydrolysis of (1) (retention time, 5.6 min) gave exclusively (2) (retention time, 3.9 min).

X-Ray Crystallography

Crystal Data.—Compound (1) C₆H₈N₂O₃S, $M = 188.2$, monoclinic, $a = 7.710(2)$, $b = 8.994(2)$, $c = 11.609(3)$ Å, $\beta = 92.10(2)^\circ$, $V = 804$ Å³, $\mu(\text{Cu-K}\alpha) = 33$ cm $^{-1}$, $\lambda = 1.54178$ Å, space group $P2_1/a$, $Z = 4$, $D_c = 1.56$ g cm $^{-3}$, $F(000) = 392$, approximate crystal dimensions $0.50 \times 0.38 \times 0.30$ mm. Compound (2) C₅H₈N₂O₂S, $M = 160.2$, monoclinic, $a = 8.530(3)$, $b = 8.136(2)$, $c = 10.700(2)$ Å, $\beta = 104.66(2)^\circ$, $V = 718$ Å³, $\mu(\text{Cu-K}\alpha) = 35$ cm $^{-1}$, $\lambda = 1.54178$ Å, space group $P2_1/c$, $Z = 4$, $D_c = 1.48$ g cm $^{-3}$, $F(000) = 336$, approximate crystal dimensions $0.27 \times 0.13 \times 0.07$ mm. Compound (4)* C₄H₆N₂O₂S, $M = 146.2$, monoclinic, $a = 9.898(2)$, $b = 5.586(1)$, $c = 21.838(4)$ Å, $\beta = 91.11(1)^\circ$, $V = 1207$ Å³, $\mu(\text{Cu-K}\alpha) = 41$ cm $^{-1}$, $\lambda = 1.54178$ Å, space group $P2_1/n$, $Z = 8$, (two crystallographically independent molecules), $D_c = 1.61$ g cm $^{-3}$, $F(000) = 608$, approximate crystal dimensions $0.17 \times 0.17 \times 0.20$ mm.

Data Collection and Processing.—(1) 1079 independent measured reflections ($\theta < 58^\circ$), 1052 observed [$|F_o| > 3\sigma|F_o|$], numerical absorption correction (face-indexed crystal); (2) 967 independent measured reflections ($\theta < 58^\circ$), 853 observed, no absorption correction; (4) 1248 independent measured reflections ($\theta \leq 50^\circ$), 1169 observed, empirical absorption correction (based on 298 azimuthal measurements). All measured on a Nicolet R3m diffractometer with Cu-K α radiation (graphite monochromator) using ω -scans.

Structure Analyses and Refinement.—All three structures were solved by direct methods and their non-hydrogen atoms were refined anisotropically. In structures (2) and (4) the positions of the NH hydrogen atoms were determined from ΔF maps and were allowed to refine isotropically. The other hydrogen atom positions, in all three structures, were idealised (C–H = 0.96 Å), assigned isotropic thermal parameters [$U(\text{H}) = 1.2U_{\text{eq}}(\text{C})$], and allowed to ride on their parent carbon atoms. Refinement was by block-cascade full-matrix least-squares and converged to give for (1) $R = 0.038$, $R_w = 0.053$ [$w^{-1} = \sigma^2(F) + 0.00096F^2$], for (2) $R = 0.044$, $R_w = 0.051$ [$w^{-1} = \sigma^2(F) +$

* When we determined the structure of compound (4), we were unaware that another determination of the structure of this molecule had recently been reported.⁶ Interestingly this other analysis is of a different polymorphic form, it has a totally different unit cell and space group, unrelated to that which we have found. Although in both structures the molecules are hydrogen-bonded to form continuous chains, in (4) there are two crystallographically independent molecules in the asymmetric unit and notable differences in the hydrogen-bonding between the two independent molecules and that linking them to their symmetry-equivalent neighbours, whilst in the other structure there is only one molecule in the asymmetric unit and the corresponding hydrogen-bonding is the same for all molecules. Also, the packing of the chains of molecules is totally different relative to the unique crystallographic b -axis in one structure compared with the other. However, there are no significant differences between the average bond lengths for the two molecules in (4) and those for the other determination.

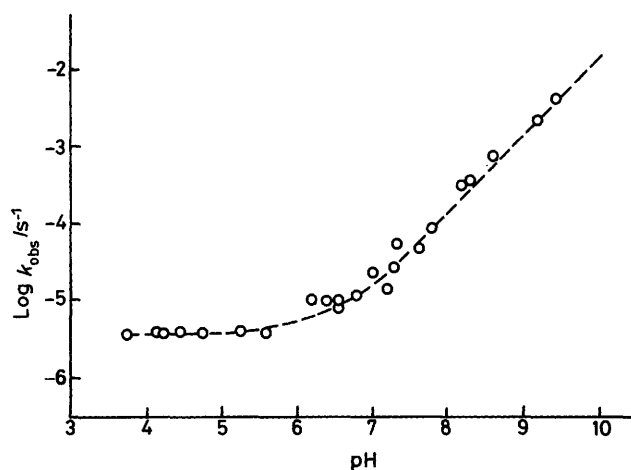


Figure 2. pH–Rate for the hydrolysis of (1). The points are experimental (and represent extrapolation to zero buffer concentration) and the curve is calculated using equation (1)

0.00087F²] and for (4) $R = 0.032$, $R_w = 0.038$ [$w^{-1} = \sigma^2(F) + 0.00027F^2$]. Computations were carried out on an Eclipse S140 computer using the SHELXTL program system.

Fractional atomic co-ordinates for the non-hydrogen atoms for (1), (2), and (4) are given in Tables 4, 5, and 6 respectively.

The fractional co-ordinates of the hydrogen atoms and isotropic thermal parameters and the anisotropic thermal parameters for the non-hydrogen atoms for (1), (2), and (4) have been deposited as Supplementary Data,[†] and the tables of structure factors are available from the editorial office on request.

Results and Discussions

The hydrolysis of (1) was studied at 25 °C over the pH range of 3.8–9.5. For a particular pH, the first-order rate constant k/s^{-1} was plotted against buffer concentration (Figure 1). The intercept of this plot on the y -axis gave k_{obs} , the rate constant at zero buffer concentration. The pH–rate profile for hydrolysis is described by equation (1) and is presented graphically in Figure 1.

$$k_{\text{obs}} = k_0 + k_{\text{OH}^-}[\text{OH}^-] \quad (1)$$

k_0 is the rate constant for the water-catalysed reaction while k_{OH^-} is the second-order rate constant for catalysis by hydroxide ions.

The curve in Figure 2 is calculated using equation (1) and $k_0 = 4.0 \times 10^{-6}$ s $^{-1}$ and $k_{\text{OH}^-} = 1.4 \times 10^2$ dm³ mol $^{-1}$ s $^{-1}$. The hydroxide ion activity was calculated from the relationships $[\text{OH}^-] = K_w/[\text{H}^+]$, $[\text{H}^+] = 10^{-\text{pH}}$, and $K_w = 1 \times 10^{-14}$ M². The slope (denoted by k_{cat}), of the plots of rate constants against buffer concentrations (Figure 1) gave a measure of the variation of rate with buffer species. A plot of k_{cat} (Table 1) against percentage free base (% B) gave the second-order rate constant for buffer catalysis, denoted by k_B (Table 2). Over the range of buffers studied only catalysis by the basic component of the buffer was significant. The second-order rate constants k_B are correlated in a linear manner (correlation coefficient $r = 0.97$) to the $\text{p}K_a$ of the buffer by the Brønsted equation, with a coefficient $\beta = 0.53 (\pm 0.14)$ (Figure 3). The positive deviation

[†] *Supplementary data* (see section 5.6.3 of Instructions for Authors, in the January issue). Hydrogen-atom co-ordinates and thermal parameters have been deposited at the Cambridge Crystallographic Data Centre.

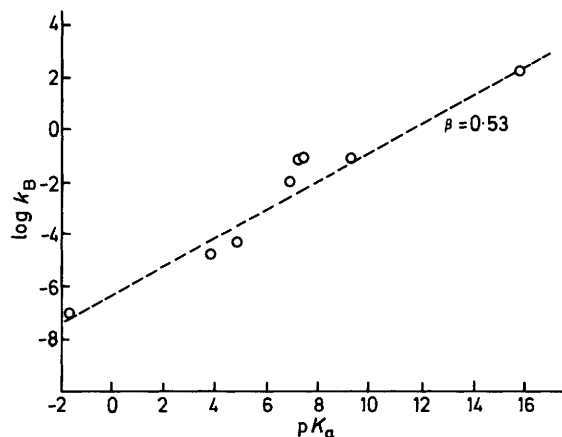
Table 1. Rate constants for the hydrolysis of (1) at 25 °C and ionic strength 1.0M

Buffer	% Free base	pH (pD)	Conc. range (mol dm ⁻³)	$k_{\text{obs}}/\text{s}^{-1}$	$k_{\text{cat}}/\text{dm}^3 \text{mol}^{-1} \text{s}^{-1}$
Formate	50	3.75	0.25—1.0	3.5×10^{-6}	0.81×10^{-5}
	70	4.16		3.8×10^{-6}	1.11×10^{-5}
	90	4.76		4.0×10^{-6}	1.42×10^{-5}
Acetate	25	4.22	0.25—1.0	4.01×10^{-6}	1.10×10^{-5}
	40	4.46		4.10×10^{-6}	1.82×10^{-5}
	50	4.57		4.00×10^{-6}	2.10×10^{-5}
	80	5.26		3.98×10^{-6}	3.00×10^{-5}
	90	5.60		3.95×10^{-6}	4.49×10^{-5}
	50	(4.78)		0.125—1.0	1.60×10^{-6}
Phosphate	19	6.21	0.01—0.1	9.18×10^{-6}	1.33×10^{-3}
	50	6.82		1.07×10^{-5}	4.15×10^{-3}
	72	7.20		1.40×10^{-5}	7.31×10^{-3}
Imidazole	25	6.37	0.003—0.01	1.01×10^{-5}	1.02×10^{-2}
	30	6.56		8.53×10^{-6}	1.81×10^{-2}
	60	7.27		2.71×10^{-5}	5.22×10^{-2}
	75	7.63		4.85×10^{-5}	6.58×10^{-2}
	90	8.19		3.00×10^{-4}	7.41×10^{-2}
<i>N</i> -Methylimidazole	10	6.45	0.005—0.02	8.98×10^{-6}	8.35×10^{-3}
	30	6.98		2.43×10^{-5}	2.27×10^{-2}
	50	7.32		5.68×10^{-5}	3.72×10^{-2}
	70	7.77		7.20×10^{-5}	5.73×10^{-2}
	90	8.33		3.14×10^{-4}	7.44×10^{-2}
Borate	20	8.65	0.003—0.01	6.76×10^{-4}	1.78×10^{-2}
	50	9.22		1.81×10^{-3}	4.18×10^{-2}
	60	9.45		3.77×10^{-3}	4.97×10^{-2}

Table 2. Rate constants for the catalysis of the hydrolysis of (1) by general base

General base	$\text{p}K_{\text{a}}^*$	$k_{\text{B}}/\text{dm}^3 \text{mol}^{-1} \text{s}^{-1}$
Water	-1.74	7.21×10^{-8}
Formate	3.77	1.62×10^{-5}
Acetate	4.76	5.20×10^{-5}
Phosphate	7.21	9.44×10^{-3}
Imidazole	6.95	6.15×10^{-2}
<i>N</i> -Methylimidazole	6.25	8.16×10^{-2}
Borate	9.23	7.35×10^{-2}
Hydroxide ion	15.75	140

* From W. P. Jencks and J. Regenstein, 'Handbook of Biochemistry and Molecular Biology,' ed. G. D. Fasman, C. R. C. Press, Cleveland, Ohio, 3rd edn., 1976, vol. 1, p. 205.

**Figure 3.** Brønsted plot for general base catalysis of the hydrolysis of (1)

of the imidazole and the *N*-methylimidazole points in Figure 3 may be attributed to electronic differences in the intermediates formed after attack either by 'oxy'- or by 'imidazole'-type nucleophiles.

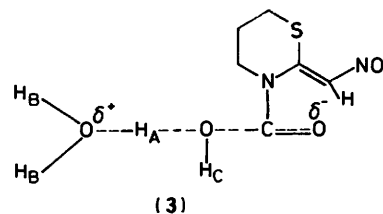
Table 3. First-order rate constants for the water-catalysed hydrolysis of (1) in H₂O-D₂O mixtures of atom fraction of deuterium 'n'

Deuterium atom fraction (<i>n</i>)	No. of runs	10 ⁶ $k_{\text{o}}^n/\text{s}^{-1}$	
		Obs.	Calc.
0.00	3	4.00	4.00
0.25	3	3.04	3.21
0.50	4	2.28	2.32
0.75	3	1.91	1.90
1.00	4	1.38	1.40

The rate of hydrolysis of (1) was also measured in 50% acetate free base (anhydrous sodium acetate and DCl were used to prepare the buffers) in D₂O and in mixtures of D₂O-H₂O. The rate constant at zero buffer concentration was found to decrease with an increase of the deuterium atom fraction, (*n*). These results could be explained⁴ using an appropriate form of the Gross-Butler equation (2) where k_{o}^n is the rate constant at a

$$k_{\text{o}}^n = k_{\text{o}}(1 - n + n\varphi_{\text{A}})(1 - n + n\varphi_{\text{B}})^2 \quad (2)$$

particular *n*, and φ_{A} and φ_{B} are the fractionation factors for H_A and H_B in the transition state (3). The fractionation factor for proton H_C is assumed to remain unity as it undergoes transition from a water to an alcohol-type proton.



The data in Table 3 give $\varphi_{\text{A}} = 0.51$ and $\varphi_{\text{B}} = 0.83$. These values are each very similar to ones reported² for the hydrolysis of the 1-acetyl-3-methylimidazolium ion. This φ_{A} value is also of

Table 4. Atomic co-ordinates ($\times 10^4$), bond lengths (\AA), and bond angles ($^\circ$) for (1)

Atom	x	y	z
S(1)	7 477(1)	3 621(1)	6 246(1)
C(2)	7 150(4)	5 591(3)	6 084(2)
C(3)	8 774(4)	6 443(3)	6 390(3)
C(4)	9 350(4)	6 283(2)	7 629(3)
N(5)	8 586(2)	4 978(2)	8 197(2)
C(6)	8 408(3)	3 615(2)	7 630(2)
C(7)	8 937(3)	2 383(2)	8 214(2)
N(8)	8 685(3)	939(2)	7 790(2)
O(1)	7 898(2)	748(2)	6 852(2)
O(2)	9 274(3)	-103(2)	8 365(2)
C(9)	8 121(3)	5 109(3)	9 316(2)
O(9)	8 356(3)	6 227(2)	9 880(2)
S(1)-C(2)	1.799(3)	S(1)-C(6)	1.736(2)
C(2)-C(3)	1.500(4)	C(3)-C(4)	1.497(4)
C(4)-N(5)	1.480(3)	N(5)-C(6)	1.396(3)
N(5)-C(9)	1.364(3)	C(6)-C(7)	1.354(3)
C(7)-N(8)	1.399(3)	N(8)-O(1)	1.239(3)
N(8)-O(2)	1.228(3)	C(9)-O(9)	1.211(3)
C(2)-S(1)-C(6)	98.7(1)	S(1)-C(2)-C(3)	111.5(2)
C(2)-C(3)-C(4)	113.2(3)	C(3)-C(4)-N(5)	113.3(2)
C(4)-N(5)-C(6)	121.4(2)	C(4)-N(5)-C(9)	118.6(2)
C(6)-N(5)-C(9)	120.0(2)	S(1)-C(6)-N(5)	117.7(1)
S(1)-C(6)-C(7)	124.9(2)	N(5)-C(6)-C(7)	117.4(2)
C(6)-C(7)-N(8)	123.3(2)	C(7)-N(8)-O(1)	119.6(2)
C(7)-N(8)-O(2)	118.3(2)	O(1)-N(8)-O(2)	122.1(2)
N(5)-C(9)-O(9)	123.2(2)		

Table 5. Atomic co-ordinates ($\times 10^4$), bond lengths (\AA), and bond angles ($^\circ$) for (2)

Atom	x	y	z
S(1)	1 033(1)	413(1)	7 423(1)
C(2)	3 146(4)	412(4)	7 437(3)
C(3)	3 662(4)	2 033(5)	6 964(3)
C(4)	2 764(4)	2 411(4)	5 607(3)
N(5)	1 019(3)	2 456(3)	5 447(3)
C(6)	164(3)	1 698(3)	6 132(3)
C(7)	-1 508(4)	1 836(4)	5 915(3)
N(8)	-2 455(3)	2 783(3)	4 980(3)
O(1)	-3 941(3)	2 863(4)	4 889(2)
O(2)	-1 857(3)	3 579(3)	4 209(2)
S(1)-C(2)	1.799(4)	S(1)-C(6)	1.741(3)
C(2)-C(3)	1.517(5)	C(3)-C(4)	1.492(5)
C(4)-N(5)	1.456(4)	N(5)-C(6)	1.311(4)
C(6)-C(7)	1.391(4)	C(7)-N(8)	1.356(4)
N(8)-O(1)	1.248(3)	N(8)-O(2)	1.254(4)
C(2)-S(1)-C(6)	103.4(1)	S(1)-C(2)-C(3)	111.8(2)
C(2)-C(3)-C(4)	112.6(3)	C(3)-C(4)-N(5)	112.1(3)
C(4)-N(5)-C(6)	128.3(3)	S(1)-C(6)-N(5)	122.7(2)
S(1)-C(6)-C(7)	113.2(2)	N(5)-C(6)-C(7)	124.1(2)
C(6)-C(7)-N(8)	124.3(3)	C(7)-N(8)-O(1)	119.4(3)
C(7)-N(8)-O(2)	120.9(3)	O(1)-N(8)-O(2)	119.7(2)

the right order of magnitude⁵ for a proton 'in flight' and is in agreement with the Brønsted coefficient β for the general base catalysis. The mechanism of hydrolysis of (1) therefore involves a transition state where a water molecule acts as a nucleophile, activated by a basic species B, which can be another water molecule.

In order to explore the reactivity of (1) we examined its crystal structure and that of (2), its product of hydrolysis. The respective molecular structures resulting from X-ray diffraction studies, together with the numbering of the various atoms, are

Table 6. Atomic co-ordinates ($\times 10^4$), bond lengths (\AA), and bond angles ($^\circ$) for (4)

Atom	x	y	z
S(1)	4 301(1)	2 187(2)	364(1)
C(2)	2 745(3)	1 593(6)	-53(2)
C(3)	1 800(3)	3 667(6)	46(1)
N(4)	2 352(2)	5 030(4)	554(1)
C(5)	3 603(3)	4 594(5)	732(1)
C(6)	4 258(3)	5 982(5)	1 168(1)
N(7)	5 560(2)	5 612(5)	1 342(1)
O(1)	6 119(2)	6 964(5)	1 728(1)
O(2)	6 224(2)	3 911(4)	1 121(1)
S(1')	1 234(1)	14 032(2)	2 229(1)
C(2')	466(3)	16 530(6)	2 621(1)
C(3')	-999(3)	16 643(6)	2 429(1)
N(4')	-1 207(2)	14 976(4)	1 931(1)
C(5')	-214(3)	13 514(5)	1 804(1)
C(6')	-381(3)	11 721(5)	1 364(1)
N(7')	604(2)	10 148(4)	1 229(1)
O(1')	357(2)	8 538(4)	836(1)
O(2')	1 750(2)	10 262(4)	1 481(1)
S(1)-C(2)	1.805(3)	S(1)-C(5)	1.719(3)
C(2)-C(3)	1.507(5)	C(3)-N(4)	1.445(4)
N(4)-C(5)	1.314(3)	C(5)-C(6)	1.379(4)
C(6)-N(7)	1.353(4)	N(7)-O(1)	1.253(4)
N(7)-O(2)	1.257(4)	S(1')-C(2')	1.813(3)
S(1')-C(5')	1.717(3)	C(2')-C(3')	1.503(4)
C(3')-N(4')	1.443(4)	N(4')-C(5')	1.312(3)
C(5')-C(6')	1.395(4)	C(6')-N(7')	1.349(4)
N(7')-O(1')	1.263(3)	N(7')-O(2')	1.253(3)
C(2)-S(1)-C(5)	91.9(1)	S(1)-C(2)-C(3)	108.2(2)
C(2)-C(3)-N(4)	106.8(3)	C(3)-N(4)-C(5)	118.0(2)
S(1)-C(5)-N(4)	113.1(2)	S(1)-C(5)-C(6)	125.1(2)
N(4)-C(5)-C(6)	121.8(3)	C(5)-C(6)-N(7)	122.7(3)
C(6)-N(7)-O(1)	120.2(3)	C(6)-N(7)-O(2)	120.7(3)
O(1)-N(7)-O(2)	119.1(2)	C(2')-S(1')-C(5')	91.8(1)
S(1')-C(2')-C(3')	108.2(2)	C(2')-C(3')-N(4')	107.8(2)
C(3')-N(4')-C(5')	117.7(2)	S(1')-C(5')-N(4')	113.7(2)
S(1')-C(5')-C(6')	125.4(2)	N(4')-C(5')-C(6')	120.9(2)
C(5')-C(6')-N(7')	122.8(2)	C(6')-N(7')-O(1')	118.7(2)
C(6')-N(7')-O(2')	121.5(2)	O(1')-N(7')-O(2')	119.2(2)

shown in Figures 4 and 5. Selected bond lengths, bond angles, and torsion angles are given in Tables 4, 5 and 7. A difference between structures (1) and (2) occurs in the nitroamine entity; crystallisation of (1) and (2) gave the *E*- and the *Z*-isomer, respectively. For the following discussion we have assumed that the position of the nitro group does not have a significant effect on the structural properties that will be considered. For both compounds the nitro group is almost in the same plane as the ethylenic group. Moreover, a comparison of the relevant structural features of (2) with the average values for the two crystallographically independent molecules of the *E*-isomer of the five-membered nitroamine heterocycle (4) (Figure 6 and Tables 6 and 7) reveals that the conjugative properties of the two molecules are similar.

The lone pair of electrons on the heterocyclic nitrogen of (1) can delocalise either in the direction of the formyl group or in

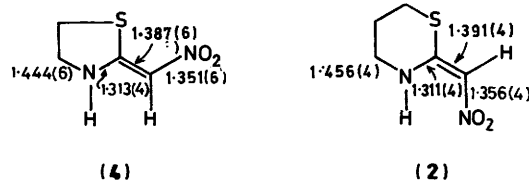


Table 7. Selected torsion angles (°)

	(1)	(2)	(4)*
C(6)-N(5)-C(9)-O(9)	174.6(2)	—	—
C(9)-N(5)-C(6)-C(7)	-44.2(3)	—	—
N(5)-C(6)-C(7)-N(8)	173.9(2)	-0.8(5)	N(4)-C(5)-C(6)-N(7) 177.7(3) -178.5(3)
C(6)-C(7)-N(8)-O(1)	-2.2(3)	-177.8(3)	C(5)-C(6)-C(7)-O(1) 178.1(3) 178.1(3)
C(6)-C(7)-N(8)-O(2)	177.1(2)	2.1(5)	C(5)-C(6)-C(7)-O(2) -2.0(4) -2.3(4)
C(7)-C(6)-N(5)-C(4)	132.8(2)	179.1(3)	C(6)-C(5)-N(4)-C(3) 172.8(3) 174.6(3)

* Two values for the two crystallographically independent molecules

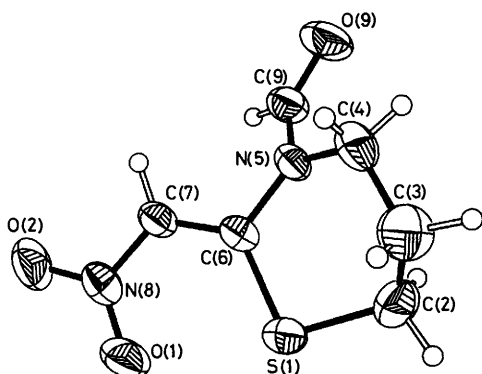


Figure 4. Molecular structure of (1) (50% probability ellipsoids) showing crystallographic numbering scheme. S(1)···O(1) 2.69 Å. There is a possible weak intermolecular C-H···O interaction between C(7) and O(9), 3.24 Å, H···O 2.38 Å, CH···O angle 149°

Table 8. Standard distances (Å) of some groups

C-N (amine)	1.471	C-N (cyclic tertiary amide)	1.336
C=N (imine)	1.330	C=O (amide)	1.234
C=C (alkene)	1.336	C=O (ketone)	1.229
C-O (alcohol)	1.426		

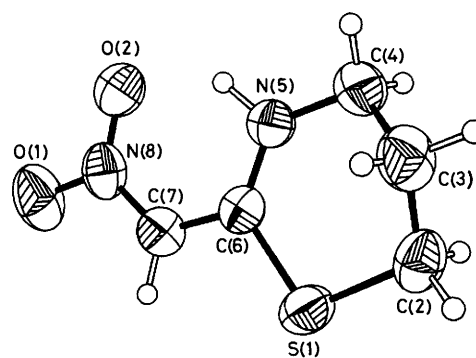
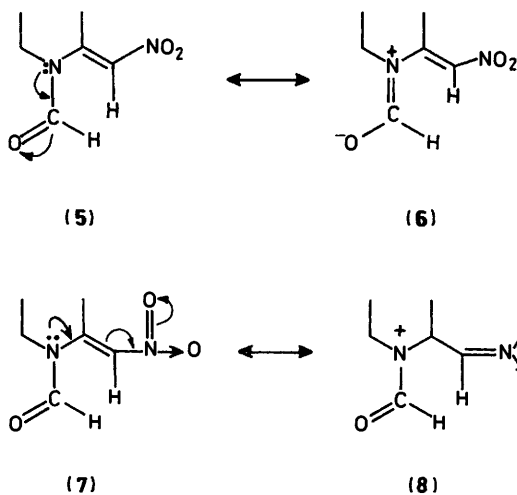


Figure 5. Molecular structure of (2) (50% probability ellipsoids) showing crystallographic numbering scheme. There is an intramolecular hydrogen bond between N(5) and O(2), 2.64 Å, H···O 1.81 Å, CH···O angle 140°.



that of the nitroamine system, giving rise to the resonance equilibria (5)–(6) and (7)–(8).

Resonance with the carbonyl group usually confers stability to amides.² In fact, the length of the C–N bond in amides⁷ is about 1.336 Å which is close to C=N in imines (Table 8). On the other hand, the length of a C=O bond in amides is slightly longer than a C=O bond in ketones but, as expected, appreciably shorter than the C–O bond in alcohols. In the case of structure (1) the amide C–N [1.364(3) Å] and the C=O [1.211(3) Å] bonds are each, respectively, longer and shorter than those expected⁷ for a cyclic tertiary amide. This indicates that delocalisation of the nitrogen lone pair into the carbonyl function is operating less effectively, mainly due to the presence of the nitroamine system. A measure of the extent to which the nitrogen lone pair is tied up in resonance (2) can be obtained

by examination of the bond lengths N(5)–C(6), C(6)–C(7), and C(7)–N(8). The length of the N(5)–C(6) [1.396(3) Å] bond lies midway between that of C–N (amine) (1.471 Å) and C=N (imine) (1.330 Å) indicating that the nitrogen lone pair is about equally delocalised in the direction of the formyl and the nitroamine groups. In comparison, the length of the equivalent bond in (2) [1.311(4) Å] shows that, as expected, the nitrogen lone pair in this molecule is wholly tied up in this nitroamine system. This is also confirmed on comparison of other equivalent bond lengths in structures (1) and (2), that is, C(6)–C(7), 1.354(3) *cf.* 1.391(4) Å and C(7)–N(8), 1.399(3) *cf.* 1.356(4) Å. These observations lead to the conclusion that the amide nitrogen atom in (1) has appreciable 'sp³' character unlike the equivalent nitrogen in (2) which is more 'sp²' in character. Moreover, examination of the C(4)–N(5)–C(6)–C(7) torsion angle in (1), 132.8(2)° with that in (2), 179.1(3)° again confirms the nearly planar nature of this part of the nitromethylene heterocycle in (2) and not in (1).

Another molecular feature of compound (1) is that the formyl group is rotated 39° out of the plane of the nitroamine system. Besides the electronic effects already discussed, it was found using molecular graphics that in a planar conformation the van der Waal radii of the formyl hydrogen [H(9)] and the enamine hydrogen [H(7)] overlap considerably and steric strain is released by the amide twisting 39° out-of-plane, with some lengthening of the N(5)–C(9) bond. This situation is similar to that described by Bieri and Viscontini⁸ in their study of the structure of a formylpterin derivative. These authors found that the formyl groups twisted out of plane of the aromatic system

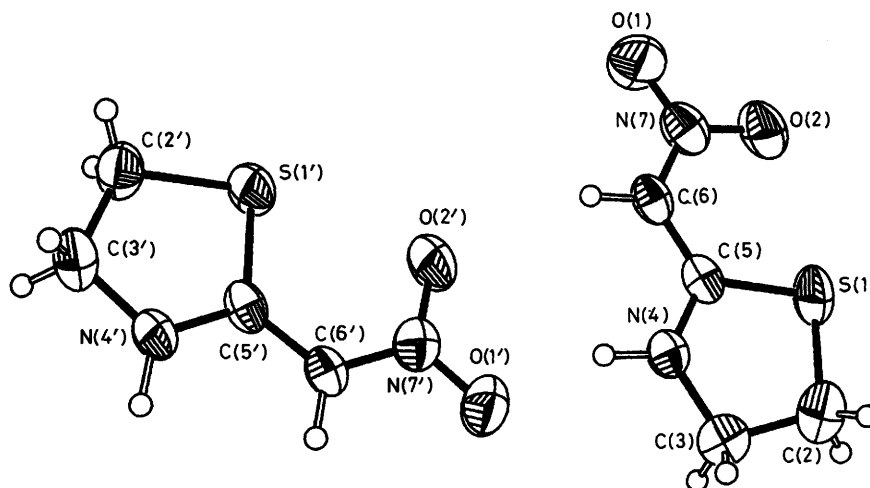
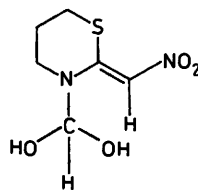


Figure 6. Two crystallographically independent molecules of (4) (50% probability ellipsoids) showing the numbering scheme. $S(1) \cdots O(2)$ 2.68 Å, $S(1') \cdots O(2')$ 2.72 Å. Hydrogen-bonding geometries: $N(4) \cdots O(1')$ 2.86, $H(4) \cdots O(1')$ 1.92 Å, $NH \cdots O$ angle 148°. To symmetry-related pair of molecules $N(4') \cdots O(1)$ 2.90, $H(4') \cdots O(1)$ 2.14 Å, $NH \cdots O$ angle 133°; $N(4') \cdots O(2)$ 3.13, $H(4') \cdots O(2)$ 2.17 Å, $NH \cdots O$ angle 165°. The $N(4) \cdots O(2')$ distance is 3.61 Å.

due to interaction of its hydrogen atom with a carbonyl oxygen 'syn' to the formyl group.

Compounds (1) and (2) may have different structural features in the solid state compared with those in solution. However, the existence of resonance structures (6) and (8) becomes more possible in an aqueous environment due to stabilisation by solvation. In this way, the crystal structure analysis outlined in this paper can be important in understanding the steps involved in the hydrolysis of (1). To summarise, some molecule factors which are thought to contribute to the hydrolytic reactivity of (1) are (i) the amide group is twisted (5.3°) from the idealised planar conformation; (ii) the C–N amide bond is longer than found in ordinary amides; (iii) the formyl group is out of plane from the nitroenamine system; and (iv) the heterocyclic ring is under some strain and hydrolysis gives the relatively less strained (2). A knowledge of the structural characteristics of (1) and (2) also allows speculation on the rapidity of the decomposition of the tetrahedral intermediate (9). The bonding nature of this intermediate is expected to resemble (2) rather



(9)

than (1). Moreover, the rationale adopted in interpreting the molecular structures of (1) and (2) leads us to believe that the C–N bond in (8) is long and weak due to the partial positive

nature of the carbon and nitrogen atoms. Moreover, before breakdown to (2) can occur, it is possible for the heterocyclic nitrogen to form a hydrogen bond with either a molecule of water or perhaps even with one of the hydroxy groups of the tetrahedral intermediate. During the course of the cleavage, the heterocyclic nitrogen increases its basic nature, leading at the same time to the shortening and strengthening of the nitrogen–hydrogen bond until this becomes a full bond.

Acknowledgements

We are indebted to Drs. A. J. Kirby, L. J. Mulheirn, and H. S. Rzepa for helpful discussions in the preparation of this manuscript.

References

- (a) B. C. Challis and J. A. Challis, 'The Chemistry of Amides,' ed. J. Zabicky, Interscience (London), 1970, 816; (b) J. Hine, R. S. M. King, W. R. Midden, and A. Sinha, *J. Org. Chem.*, 1981, **46**, 3186.
- D. G. Oakenfull and W. P. Jencks, *J. Am. Chem. Soc.*, 1971, **93**, 178.
- R. L. Schowen, H. Jazaraman, and L. Kershner, *J. Am. Chem. Soc.*, 1966, **88**, 3373.
- R. L. Ehrhardt, G. Gopalakrishnan, and J. L. Hogg, *J. Org. Chem.*, 1983, **48**, 1586.
- W. J. Albery, 'Proton Transfer Reactions,' eds. E. Galdin and V. Gold, Chapman and Hall, London, 1975.
- S. Rajapa, K. Nagarajan, K. Venkatesan, N. Kamath, V. M. Padmanabhan, W. von Philipborn, B. C. Chen, and R. Muller, *Helv. Chim. Acta*, 1984, **67**, 1669.
- P. Chakrabarti and J. P. Dunitz, *Helv. Chim. Acta*, 1982, **65**, 1555.
- J. H. Bieri and M. Viscontini, *Helv. Chim. Acta*, 1977, **60**, 447.

Received 22nd June 1987; Paper 7/1117